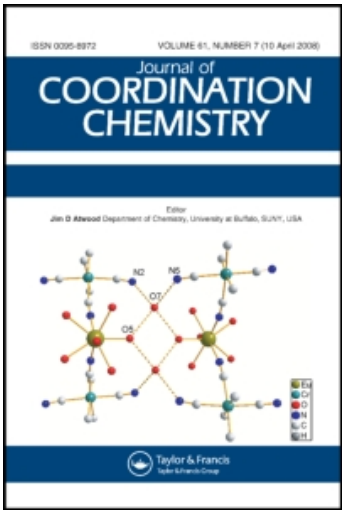

Journal of Coordination Chemistry
Publication details, including instructions for authors and subscription information:
http://www.informaworld.com/smpp/title~content=t713455674

Synthesis, structure, and complexation properties of hydroxybenzyl analogs of diethylenetriaminepentaacetic acid

Henna Pesonen[a]; Anna Wuorimaa[b]; Reija Jokela[b]; Reijo Aksela[c]; Kari Laasonen[a]
[a] Department of Chemistry, University of Oulu, 90014 Oulu, Finland [b] Laboratory of Industrial Chemistry, Helsinki University of Technology (TKK), 02015 Espoo, Finland [c] Espoo Research Centre, 02271 Espoo, Finland

First published on: 13 July 2010

To cite this Article Pesonen, Henna , Wuorimaa, Anna , Jokela, Reija , Aksela, Reijo and Laasonen, Kari(2010) 'Synthesis, structure, and complexation properties of hydroxybenzyl analogs of diethylenetriaminepentaacetic acid', Journal of Coordination Chemistry, 63: 12, 2026 — 2041, First published on: 13 July 2010 (iFirst)
To link to this Article: DOI: 10.1080/00958972.2010.499936
URL: http://dx.doi.org/10.1080/00958972.2010.499936

Journal of Coordination Chemistry
Vol. 63, No. 12, 20 June 2010, 2026–2041

Taylor & Francis
Taylor & Francis Group

Synthesis, structure, and complexation properties of hydroxybenzyl analogs of diethylenetriaminepentaacetic acid

HENNA PESONEN†, ANNA WUORIMAA‡, REIJA JOKELA‡, REIJO AKSELA§ and KARI LAASONEN*†

†Department of Chemistry, University of Oulu, PO Box 3000, 90014 Oulu, Finland
‡Laboratory of Industrial Chemistry, Helsinki University of Technology (TKK), PO Box 6100, 02015 Espoo, Finland
§Espoo Research Centre, Kemira Oyj, PO Box 44, 02271 Espoo, Finland

(*Received 22 December 2009; in final form 22 April 2010*)

As part of continuous search for new chelating agents for transition metal ions, a practical method for the preparation of hydroxybenzyl derivatives of diethylenetriaminepentaacetic acid (DTPA) has been developed in this study. *N*,*N*″-bis(2-hydroxybenzyl)diethylenetriamine-*N*,*N*′,*N*″-triacetic acid (HBDTTA) and four other hydroxybenzyl derivatives of DTPA have been synthesized. The structures and chelating capacity of three ligands with Fe^{3+} have been predicted using density functional theory-based calculations at the BP86/TZVP level within a previously developed and tested computational procedure. The results show that like DTPA, HBDTTA can adopt several different six- and seven-coordinate complex structures. The good stability of Fe^{3+} complexes of two HBDTTA derivatives indicates that HBDTTA-type ligands can be modified by removing some of their functional groups without greatly affecting their metal-binding efficiency.

Keywords: DTPA; HBDTTA; Complexation; Iron; DFT

1. Introduction

For environmental reasons, pulping methods based on oxygen chemicals, for example hydrogen peroxide and peroxy acids have become popular. Transition metal ions, especially Fe^{3+} and Mn^{2+}, catalyze the decomposition of hydrogen peroxide [1, 2]. Thus, their removal from bleaching liquors by chelation is an essential step in the bleaching sequences. Commonly used complexing agents in such chelation steps are ethylenediaminetetraacetic acid (EDTA) and diethylenetriaminepentaacetic acid (DTPA) (figure 1) [3]. These ligands are well-known and effective chelating agents for transition metal ions. However, during the past decades, the environmental fate of such ligands has become an issue. The possible ability of chelating agents to mobilize heavy metals from the sediments is one of their environmental drawbacks.

As a result of continuous search for environmentally benign complexing agents, we have introduced a series of green alternatives for EDTA and DTPA [4–11].

*Corresponding author. Email: kari.laasonen@oulu.fi

ISSN 0095-8972 print/ISSN 1029-0389 online © 2010 Taylor & Francis
DOI: 10.1080/00958972.2010.499936

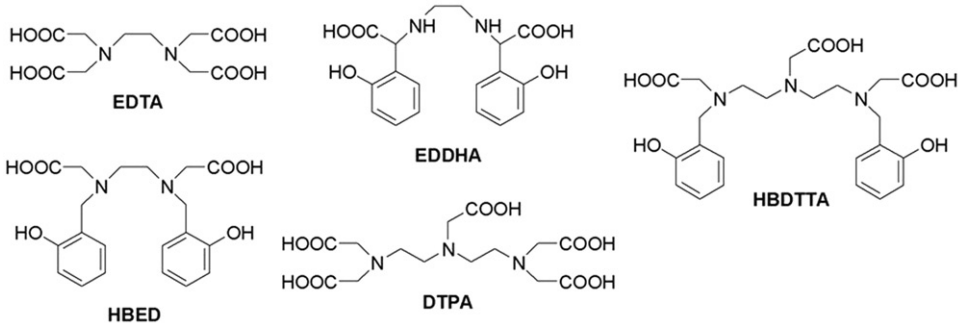

Figure 1. Structures of commonly known complexing agents.

However, despite their high stability constants, the performance of complexing agents is not always satisfactory in deactivating iron and manganese ions in hydrogen peroxide solutions. In fact, some metal complexes are able to catalyze the decomposition of the peroxy compounds [12]. At this point, it becomes very important to know the detailed structure of each complex. Furthermore, by studying the relative stability of different conformations, the performance of the ligands can be better understood both in bleaching processes and other applications.

Replacement of the carboxymethyl groups of EDTA with 2-hydroxybenzyl groups has increased the affinities of the ligands for some trivalent metal ions. Examples of such compounds are *N*,*N*′-bis(2-hydroxybenzyl)ethylenediamine-*N*,*N*′-diacetic acid [13] (HBED, figure 1) and ethylenediamine di(*o*-hydroxyphenylacetic acid) [14] (EDDHA, figure 1), which are known for their strong ability to bind metal ions like Fe^{3+}. Also, DTPA is known to be an excellent chelating agent. Recently, an analog of DTPA, *N*,*N*″-bis(2-hydroxybenzyl)diethylenetriamine-*N*,*N*′,*N*″-triacetic acid (HBDTTA, figure 1) and its stability constants with several metal ions have been introduced [15, 16].

Molecular modeling has become an efficient tool in ligand study and design. By utilizing powerful modeling tools, the development time of new ligands can be significantly reduced. Moreover, the volume of chemicals can be decreased due to fewer syntheses and application tests. In the previous work [17], we studied the complexation properties of various amino polycarboxylic acids, including, for example, EDTA, DTPA, AES, and ISA using density functional methods (DFT), a continuum solvation model (COSMO, conductor-like screening model) and Car–Parrinello *ab initio* molecular dynamics. As a result, a fast and straightforward computational method for evaluating the performance of complexing agents was developed. The method has been further tested with oligomeric ligands [17, 18] as well as with other amino polycarboxylic acid ligands [19]. The results (binding trends and complexation geometries) were promising compared to the available experimental data. Recently, we have applied the method to study the complexation properties of cysteine [20].

Here, we report the syntheses of HBDTTA, *N*,*N*″-bis(2-hydroxybenzyl) diethylenetriamine-*N*,*N*′,*N*″-tri-2-propionic acid (HBDTTP), and three other hydroxybenzyl derivatives of DTPA. For three ligands, complexation geometries and energies with Fe^{3+} have been determined with DFT (BP86/TZVP) and COSMO solvation model. The results have been compared to DTPA as well as to other commonly known

chelating agents, such as EDTA. In summary, in this study, molecular modeling has been used to predict the complexation behavior of completely new ligands within the previously developed and tested computational procedure [17]. Applicability of the ligands is discussed with special attention to pulp bleaching processes.

2. Experimental

Infrared spectra were recorded on a Perkin–Elmer Spectrum One FT-IR. NMR spectra were recorded on a Bruker AV-400 spectrometer. Chemical shifts (δ) are reported in ppm relative to TMS (^{1}H-NMR; $\delta_H = 0.00$ ppm) and $CDCl_3$ (^{13}C-NMR; $\delta_C = 77.000$ ppm). Signal assignments are based on standard HSQC and ^{1}H-^{1}H COSY experiments. Mass spectra (EI and HRMS, 70 eV, m/z) were obtained on a Jeol DX 303/DA 5000 instrument. Mass spectra of compounds **3*b**, **4*c**, **e**, and **5*d** were obtained on a Micromass LCT TOF MS (ES+) instrument.

All compounds were purified by column chromatography (CH_2Cl_2 : MeOH, 99.5 : 0.5) using Merck Kieselgel 60 (230–400 mesh).

2.1. *Preparation of N,N″-bis(2-hydroxybenzyl)diethylene triamine (1)*

Salicylaldehyde (0.2 mol) was added to a solution of diethylenetriamine (0.1 mol) in 99.5% ethanol (120 mL). After stirring for 3 h at room temperature, $NaBH_4$ (0.22 mol) was added in small portions during 30 min at 0°C. After 4 h, the mixture was poured into H_2O (110 mL) and extracted with CH_2Cl_2. The extracts were washed with 5% $NaHCO_3$, dried over Na_2SO_4, and evaporated *in vacuo*.

2.1.1. *N,N″*-bis(2-hydroxybenzyl)diethylenetriamine (1). Amorphous; ^{1}H-NMR (400 MHz; $CDCl_3$) δ_H 2.65–2.71 (8H, m), 3.90 (4H, s), 6.74 (2H, t, $J = 7.5$ Hz), 6.77 (2H, d, $J = 7.5$ Hz), 6.95 (2H, d, $J = 7.5$ Hz), 7.11 (2H, t, $J = 7.5$ Hz); ^{13}C-NMR (100 MHz; $CDCl_3$) δ_C 47.6 (2C), 48.1 (2C), 51.9 (2C), 115.9 (2C), 118.7 (2C), 122.4 (2C), 128.2 (2C), 128.3 (2C), 157.7 (2C); m/z (EI) 315 (M^+), 136, 107(100%). Exact mass: 315.1950 (Calcd for $C_{18}H_{25}N_3O_2$: 315.1947).

2.2. *General procedure for the N-alkylation*

N,N″-bis(2-hydroxybenzyl)diethylenetriamine (**1**) (1.0 mmol) and *N,N*-diisopropylethylenediamine (DIPEA, 6.4 mmol) in DMF (20 mL) were mixed under argon and cooled to 0°C. The alkylating agent **2a–e** (3.5 mmol) was added during 45 min keeping the solution at 0°C. The reaction mixture was stirred at room temperature for 2 h and then at 50°C for 18 h. The reaction mixture was poured into H_2O and extracted with CH_2Cl_2. The extracts were washed with H_2O, dried over Na_2SO_4, and evaporated *in vacuo*.

The *N*-alkylation with **2a** (683 mg, 3.5 mmol) gave 526 mg of crude product comprising 368 mg of compound **3*a**.

2.2.1. *N,N″*-bis(2-hydroxybenzyl)diethylenetriamine-*N,N′,N″*-triacetic acid *tert*-butyl ester (3*a). Amorphous, FT-IR 1731 (CO); ^{1}H-NMR (400 MHz; $CDCl_3$) δ_H 1.41 (9H, s), 1.46 (18H, s), 2.69 (4H, t, $J = 7.0$ Hz), 2.78 (4H, t, $J = 7.0$ Hz), 3.20 (2H, s), 3.24 (4H, s), 3.78 (4H, s), 6.74 (2H, t, $J = 7.5$ Hz), 6.81 (2H, d, $J = 7.5$), 6.94 (2H, d, $J = 7.5$ Hz), 7.15 (2H, t, $J = 7.5$ Hz); ^{13}C-NMR (100 MHz; $CDCl_3$) δ_C 27.9 (9C), 50.9 (2C), 51.3 (2C), 55.3, 55.4 (2C), 56.8 (2C), 80.9, 81.5 (2C), 116.2 (2C), 118.8 (2C), 121.8 (2C), 128.8 (2C), 129.0 (2C), 157.4 (2C), 169.9 (2C), 170.1; *m/z* (EI) 657 (M^+), 556, 301, 189 (100%), 107. Exact mass: 657.4000 (Calcd for $C_{36}H_{55}N_3O_8$: 657.3989).

The *N*-alkylation with **2b** (732 mg, 3.5 mmol) gave 429 mg of crude product comprising 265 mg of compound **3*b**. According to ^{13}C spectrum, there are four diastereomeric structures of compound **3*b**. Assignment (1C) in spectral data includes ^{13}C chemical shifts for four diastereomers.

2.2.2. *N,N″*-bis(2-hydroxybenzyl)diethylenetriamine-*N,N′,N″*-tripropionic acid *tert*-butyl ester (3*b). Amorphous; FT-IR 1725 (CO); ^{1}H-NMR (400 MHz; $CDCl_3$) δ_H 1.10–1.18 (3H, m), 1.19–1.25 (6H, m), 1.41 (9H, s), 1.48 (18H, s), 2.52–2.79 (8H, m), 3.27 (1H, q, $J = 7.0$ Hz), 3.46 (2H, q, $J = 7.0$ Hz), 3.73–3.85 (4H, m), 6.74 (2H, t, $J = 7.5$ Hz), 6.79 (2H, d, $J = 7.5$), 6.93 (2H, d, $J = 7.5$ Hz), 7.13 (2H, t, $J = 7.5$ Hz); ^{13}C-NMR (100 MHz; $CDCl_3$) δ_C 12.7–13.1 (2C), 15.0–15.8 (1C), 28.1 (9C), 48.5–49.2 (2C), 49.5–50.3 (2C), 54.5–54.9 (2C), 58.1–58.4 (2C), 58.6–59.4 (1C), 80.8–80.9 (1C), 81.5–81.6 (2C), 116.2 (2C), 119.0 (2C), 121.9 (2C), 128.8–129.2 (4C), 157.7–157.8 (2C), 171.9–172.0 (2C), 172.7 (1C); *m/z* (ES+) 701 ($M^+ + 1$), 320 (100%). Exact mass: 699.4497 (Calcd for $C_{39}H_{61}N_3O_8$: 699.4459).

The *N*-alkylation with **2c** (429 mg, 3.5 mmol) gave 320 mg of crude product comprising 179 mg of compound **4*c**.

2.2.3. Piperazinone 4*c. Amorphous; FT-IR 1737 (CO), 1654 (CON); ^{1}H-NMR (400 MHz; $CDCl_3$) δ_H 1.27 (3H, t, $J = 7.0$ Hz), 2.72–2.80 (4H, m), 3.14 (2H, dd, $J = 6.0$ Hz), 3.24 (2H, s), 3.45–3.47 (2H, m), 3.49 (2H, s), 3.74 (2H, s), 3.80 (2H, s), 4.19 (2H, q, $J = 7.0$ Hz) 6.73–7.19 (8H, m); ^{13}C-NMR (100 MHz; $CDCl_3$) δ_C 14.0, 42.4, 45.4, 48.8, 49.6, 53.8, 56.4, 58.1, 60.0, 61.0, 116.2 (2C), 119.1, 119.4, 120.2, 121.6, 128.9, 129.1, 129.2, 129.5, 157.0, 157.2, 166.1, 171.0; *m/z* (ES+) 442 ($M^+ + 1$), 336 (100%), 230. Exact mass: 441.2243 (Calcd for $C_{24}H_{31}N_3O_5$: 441.2264).

The *N*-alkylation with **2d** (585 mg, 3.5 mmol) gave 481 mg of crude product comprising 192 mg of compound **3*d** and 289 mg of compound **5*d**.

2.2.4. *N,N″*-bis(2-hydroxybenzyl)diethylenetriamine-*N,N′,N″*-tripropionic acid ethyl ester (3*d). Amorphous; FT-IR 1739 (CO); ^{1}H-NMR (400 MHz; $CDCl_3$) δ_H 1.21 (3H, t, $J = 7.0$ Hz), 1.25 (6H, t, $J = 7.0$ Hz), 2.72 (4H, t, $J = 7.0$ Hz), 2.80 (4H, t, $J = 7.0$ Hz), 3.31 (2H, s), 3.34 (4H, s), 3.79 (4H, s), 4.09 (2H, q, $J = 7.0$ Hz), 4.15 (4H, q, $J = 7.0$ Hz), 6.75 (2H, t, $J = 7.5$ Hz), 6.82 (2H, d, $J = 7.5$ Hz), 6.95 (2H, d, $J = 7.5$ Hz), 7.16 (2H, t, $J = 7.5$ Hz); ^{13}C-NMR (100 MHz; $CDCl_3$) δ_C 13.7 (3C), 50.6 (2C), 50.9 (2C), 53.2 (2C), 54.2 (1C), 56.6 (2C), 59.9 (1C), 60.4 (2C), 115.8 (2C), 118.6 (2C), 121.5 (2C), 128.6 (2C), 128.9 (2C), 157.1 (2C), 170.3 (2C), 170.4 (1C); *m/z* (EI) 573 (M^+), 500, 245 (100%), 222, 107. Exact mass: 573.3007 (Calcd for $C_{30}H_{43}N_3O_8$: 573.3050).

2.2.5. Piperazinone 5*d. Amorphous; FT-IR 1739 (CO), 1650 (CON); ^{1}H-NMR (400 MHz; $CDCl_3$) δ_H 1.23 (3H, t, $J = 7.0$ Hz), 1.24 (3H, t, $J = 7.0$ Hz), 2.69 (2H, t, $J = 6.0$ Hz), 2.80 (2H, t, $J = 6.0$ Hz), 3.10 (2H, t, $J = 6.0$ Hz), 3.23 (2H, s), 3.24 (2H, s), 3.44 (2H, t, $J = 6.0$ Hz), 3.47 (2H, s), 3.77 (2H, s), 4.15 (2H, q, $J = 7.0$ Hz), 4.16 (2H, q, $J = 7.0$ Hz), 6.72 (1H, t, $J = 7.5$ Hz), 6.78 (1H, d, $J = 7.5$ Hz), 6.93 (1H, d, $J = 7.5$ Hz), 7.12 (1H, t, $J = 7.5$ Hz); ^{13}C-NMR (100 MHz; $CDCl_3$) δ_C 14.1 (2C), 42.9, 46.0, 49.0, 49.1, 54.1, 56.6, 57.8, 58.1, 60.9, 61.1, 116.3, 119.2, 121.8, 129.2, 129.5, 157.3, 166.5, 169.2, 170.7; *m/z* (ES+) 422 ($M^+ + 1$), 316 (100%), 213. Exact mass: 421.2206 (Calcd for $C_{21}H_{31}N_3O_6$: 421.2213).

The *N*-alkylation with **2e** (634 mg, 3.5 mmol) gave 458 mg of crude product comprising *ca* 300 mg of compound **4*e** (mixture of diastereomers). Assignment (1C) in spectral data includes ^{13}C chemical shifts for two diastereomers.

2.2.6. Piperazinone 4*e. Amorphous; FT-IR 1730 (CO), 1646 (CON); ^{1}H-NMR (400 MHz; $CDCl_3$) δ_H 1.30 (3H, t, $J = 7.0$ Hz), 1.37 (3H, d, $J = 7.0$ Hz), 1.51 (3H, d, $J = 7.0$ Hz), 2.56–2.67 (1H, m), 2.72–2.84 (2H, m), 3.04–3.21 (3H, m), 3.27–3.32 (1H, m), 3.38–3.46 (1H, m), 3.54–3.59 (1H, m), 3.60–3.69 (1H, m), 3.75–3.90 (2H, m), 3.96–4.05 (1H, m), 4.14–4.18 (1H, m), 4.21 (2H, q, $J = 7.0$ Hz), 6.74–6.86 (4H), 6.96–7.02 (2H), 7.13–7.20 (2H); ^{13}C-NMR (100 MHz; $CDCl_3$) δ_C 11.2–11.8 (1C), 14.1 (1C), 15.1–15.3 (1C), 43.7–43.9 (1C), 44.3–44.6 (1C), 44.7–44.8 (1C), 46.3–46.6 (1C), 53.7 (1C), 56.4–56.5 (1C), 57.0 (1C), 60.1–60.2 (1C), 60.9–61.0 (1C), 116.1–116.2 (2C), 119.0–119.3 (2C), 121.6–121.7 (2C), 128.8–129.0 (2C), 129.4–129.5 (2C), 157.2–157.3 (2C), 169.4–169.6 (1C), 172.9–173.2 (1C); *m/z* (ES+) 470 ($M^+ + 1$) 386, 364 (100%). Exact mass: 469.2577 (Calcd for $C_{26}H_{35}N_3O_5$: 469.2577).

2.3. *Computational procedure*

All geometry optimizations have been performed using the program TURBOMOLE 6.0 [21]. The optimizations have been carried out with DFT using the BP86 functional [22, 23] and all-electron triple zeta valence polarization (TZVP) basis set for all atoms. The RI approximation [24, 25] has been used to speed up the calculations. Two other density functionals, PBE0 [26] and B3LYP [27], have been tested for selected structures. All the geometries have been optimized using the COSMO solvation model [28]. Apart from the radius for Fe^{3+} ion, default options of the program TURBOMOLE have been used. The COSMO radius used for Fe^{3+} is 1.391 Å and it has been determined using a hexaaquo Fe^{3+} complex. For details of the determination of the metal radius, we refer the reader to references [17, 18]. All complexes have preferred high-spin configurations.

The complexation energies have been calculated using equation (1).

$$\Delta E_{C0} = \Delta E_{CSM} = E_{CSM}(ML^{n-m}) + 6E_{CSM}(H_2O) - E_{CSM}(M(H_2O)_6^{n+}) - E_{CSM}(L^{m-}), \quad (1)$$

E_{CSM} (X) is the COSMO-corrected total energy of species (X). Both the complex structures and the free ligands were optimized using the COSMO solvation model.

Complexation energies ΔE_{C0} offer a useful tool for comparing the relative stabilities of different structures. However, if one wants to evaluate the absolute binding strength

of the ligands, ΔE_{C0} values calculated need to be corrected as they have been shown [17] to deviate quite a lot from the experimental $\Delta G_{experimental}$ derived from $\log K$ values. In this study, we apply the previously [17] introduced effective parameterization to correct for missing contributions in complexation energies. Corrected complexation energy ΔG_{C1} is defined as

$$\Delta G_{C1}(M_i, L_j) = \Delta E_{C0}(M_i, L_j) + \tilde{G}_{MLi}, \quad (2)$$

$\tilde{G}_{MLi}$ is a metal-specific correction parameter, determined for metal complexes of amino polycarboxylic acid ligands, including, for example, EDTA and DTPA. These parameters were determined by fitting the complexation energies obtained by the DFT/COSMO approach to reproduce experimental data. The method has been successfully applied to metal complexes of oligomeric ligands [18, 29] as well as to other amino polycarboxylic acids [19] including, for example, different isomers of EDDHA. The value of $\tilde{G}_{MLi}$ depends on the used density functional. Recently [20], we tested three other density functionals for metal complexes of cysteine, and ΔE_{C0} were found to be highly dependent on the chosen functional. For EDTA, on the other hand, differences were smaller [30].

The complexation energy calculations do not include any explicit thermal or internal entropy corrections. Other missing contributions include at least corrections for ZPE, nonelectrostatic solvation effects, and basis set superposition error (BSSE). However, as accurate calculation of these contributions is very demanding and, on the other hand, as the applicability of this kind of approach has already been demonstrated in previous studies [17–20], this omission is not a concern. The magnitude of some of these contributions has been estimated for selected cases by Sillanpää *et al.* [17].

3. Results

3.1. *Synthesis of hydroxybenzyl analogs of DTPA*

We applied a commonly known procedure to synthesize *N*,*N*″-bis(2-hydroxybenzyl) diethylenetriamine (**1**) for the synthesis of salenides [31]. Addition of diethylenetriamine to salicylaldehyde followed by reduction with $NaBH_4$ (scheme 1) resulted in the formation of **1** in good yield (97%). The product was used without purification in the next *N*-alkylation step.

Five different alkylating agents (scheme 2, compounds **2a**–**e**) were chosen for the *N*-alkylation step. The influences of the ester moiety, the leaving group X and an added methyl group were studied. All the experiments were performed with equimolar ratios of starting material and identical reaction conditions (time and temperature).

In the literature [13], an inorganic base has been used in the *N*-alkylation step. However, sodium carbonate in DMF solution was unsuccessful in our hands, whereas the use of an organic base DIPEA gave good results in most cases.

In the S_N2-reactions of *N*,*N*″-bis(2-hydroxybenzyl)diethylenetriamine (**1**) with alkyl halides **2a**–**e**, formation of the corresponding trialkylated products was assumed. Indeed, this took place with alkyl halides **2a**, **2b**, and **2d**. The trialkylated products **3*a**, **3*b**, and **3*d** were formed. In addition, small amounts of dialkylated products were formed.

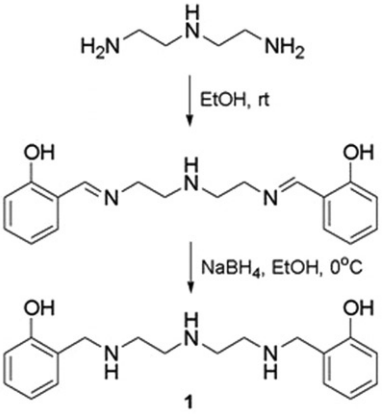

Scheme 1. Preparation of *N*,*N*′-bis(2-hydroxybenzyl)diethylenetriamine (**1**).

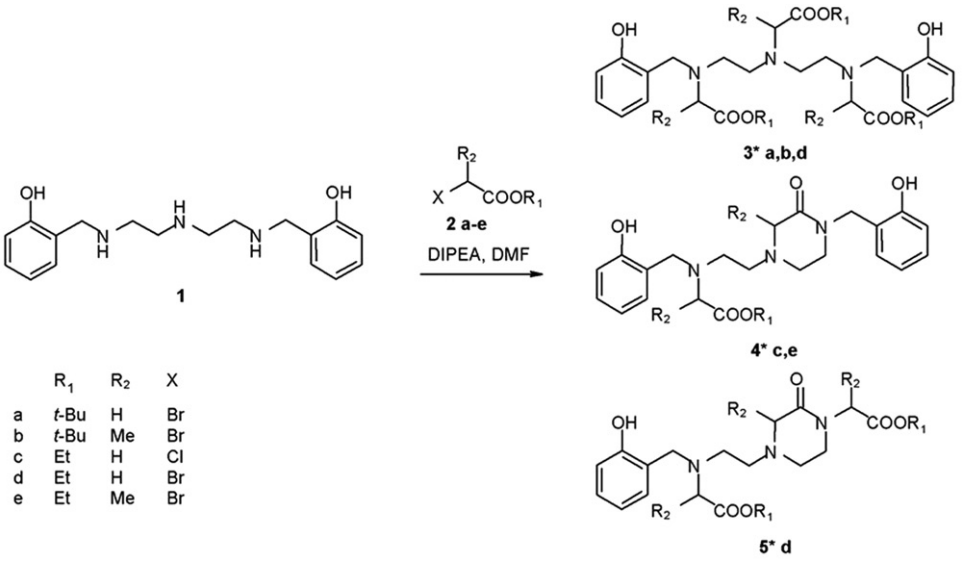

Scheme 2. Synthesis of the *N*-alkylated 2-hydroxybenzyl derivatives of diethylenetriamine.

Since the reaction of the secondary alkyl halide **2b** was significantly slower than the reaction of the primary alkyl halide **2a**, more of the dialkylated product was formed.

With dialkylated products additional ring formation was possible. Ring formation was observed with alkyl halides **2c** and **2e**. The fact that alkyl halides **2a** and **2b** yielded no cyclic products, **4*a** and **4*b** can be explained by comparing the two leaving groups. In an S_N2-reaction, a *t*-butoxy group is a poorer leaving group than an ethoxy group.

When ethyl bromoacetate **2d** was used, the cyclic compound **5*d** where one of the hydroxybenzyl groups was replaced by an alkyl group was formed. It can be explained by the formation of a quaternary ammonium salt of **4*c** from which the hydroxybenzyl group is removed more readily than the alkyl group. The formation of a quaternary salt is due to better reactivity of ethyl bromoacetate **2d** compared to ethyl chloroacetate **2c**.

As a result, an effective method for preparation of glycine and methylglycine derivatives of *N*,*N*″-bis(2-hydroxybenzyl)diethylenetriamine was developed. The reactions gave good yields when *t*-butyl esters of the alkylating agents were applied. In summary, we were able to shorten the known syntheses of HBDTTA [15, 16] by ignoring either the protection step or the amide reduction. In addition, the products were hydrolyzed in aqueous alkaline conditions to yield salts of **3a**, **3b**, **3d**, **4c**, **4e**, and **5d**.

3.2. *Geometries and relative stabilities*

As described above, the synthesis products (figure 2) may have either a methyl group or a hydrogen attached to the carbons next to the amino groups (R_2, respectively). However, as the methyl group does not coordinate with the metal, it does not directly participate in the complexation reaction. Thus, we replaced it by hydrogens simply for computational reasons.

We optimized Fe^{3+} complexes for three synthesis products. The studied ligands were HBDTTA and its two incompletely alkylated derivatives (**4c** and **5d**). In order to find the minimum energy structures, we optimized 5–8 different structures for each ligand with different coordination modes. In addition to complexes of new ligands, previously studied $[Fe–DTPA]^{2-}$ complexes were reoptimized with COSMO. All the carboxylic

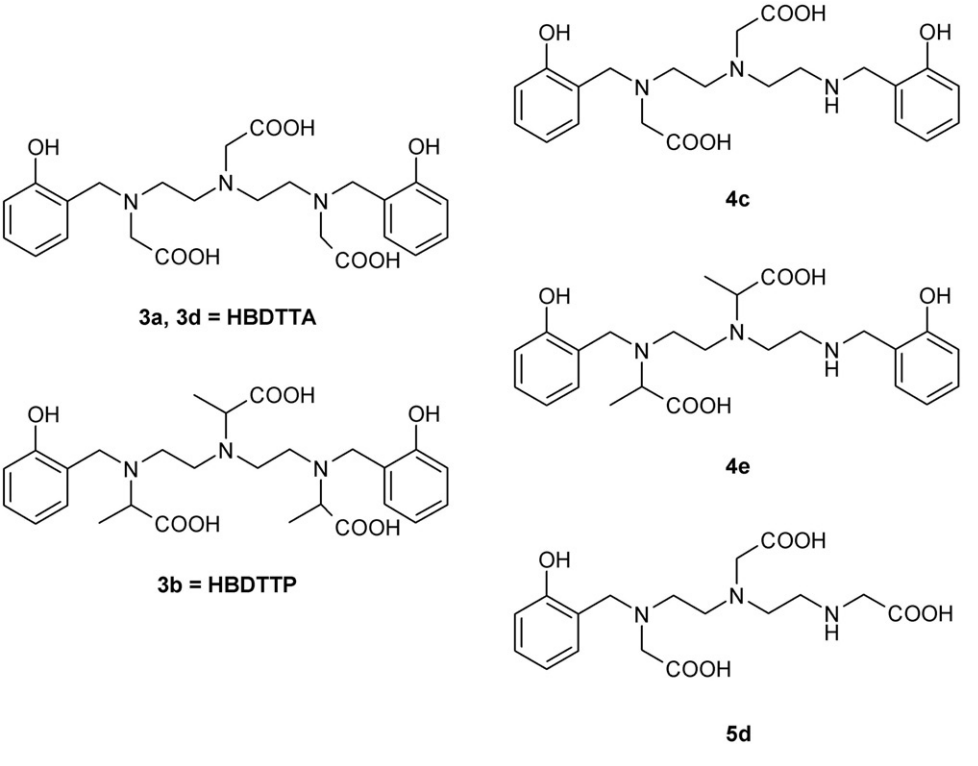

Figure 2. Synthesis products in their acid form.

acid and phenolic groups were considered completely deprotonated. The most stable structures for $[Fe–HBDTTA]^{2-}$, $[Fe–\mathbf{4c}]^{-}$, $[Fe–\mathbf{5d}]^{-}$, and $[Fe–DTPA]^{2-}$ are shown in figure 3. As the ligands were relatively flexible, figure 3 includes several structures for each complex.

In general, we found six- and seven-coordinate structures for all the ligands. Despite the fact that HBDTTA and DTPA have in total eight possible metal-coordinating atoms, eight-coordinated structures seem to be clearly higher in energy than the most stable structures [17] and in fact, no such structures were found for $[Fe–HBDTTA]^{2-}$. For $[Fe–HBDTTA]^{2-}$, six-coordinate structure **6b** is the most stable one with an energy difference of 23 kJ mol^{-1} with respect to the second best six-coordinate structure **6a** and 22 kJ mol^{-1} to the most stable seven-coordinate structure. For $[Fe–DTPA]^{2-}$, all three structures are within 7 kJ mol^{-1} and thus, considered equally stable. However, if the absolute energies are considered (see section 3.4), all modeled HBDTTA structures have clearly lower complexation energies than the lowest DTPA complexes. Note that for HBDTTA, there are several relatively stable structures with only one metal-binding phenol group and thus, the expected increase in stability with respect to DTPA does not necessarily originate from the fact that both phenol groups bind to the metal.

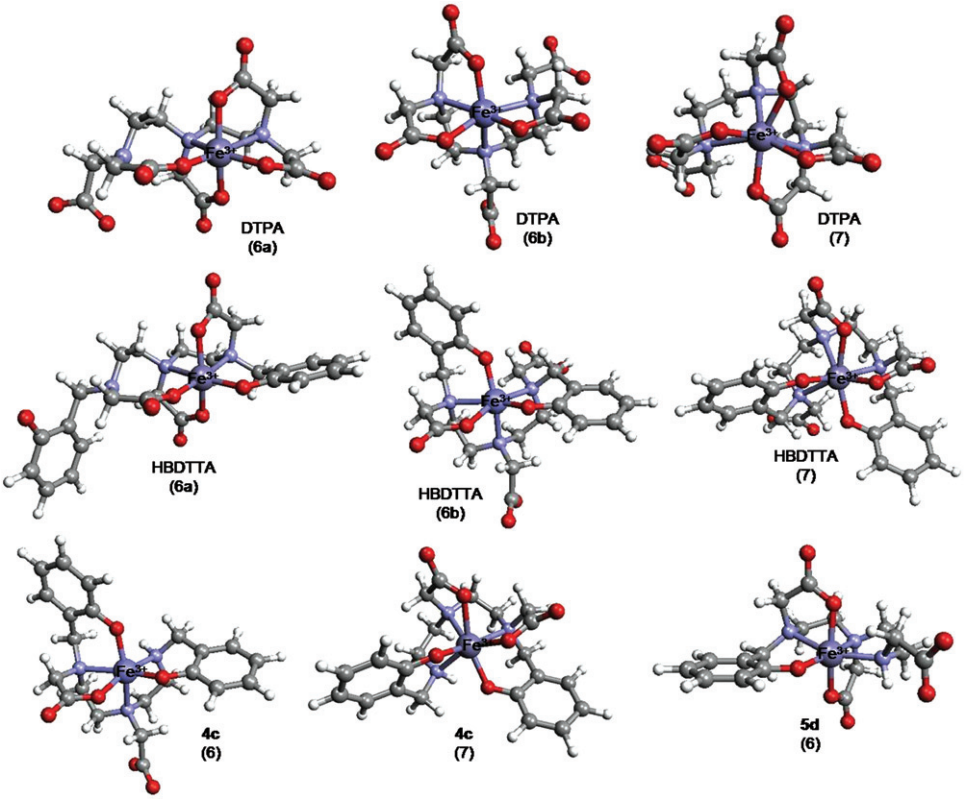

Figure 3. The most stable structures for $[Fe–HBDTTA]^{2-}$, $[Fe–\mathbf{4c}]^{1-}$, $[Fe–\mathbf{5d}]^{1-}$, and $[Fe–DTPA]^{2-}$. The structures have been optimized at the BP86/TZVP level using the COSMO solvation model.

For **4c**, the most stable structure is identical to six-coordinate structure **6b** of HBDTTA with the exception of one free COO^- group of HBDTTA complex which is absent in [Fe–**4c**]$^-$. The energy difference between the six- and seven-coordinate structures is almost identical to HBDTTA. With **5d**, the most stable structure is six-coordinate with one COO^- group pointing out to the solvent. The structures of two DTPA and HBDTTA complexes are compared in more detail in the following section.

In general, all the ligands were shown to be quite flexible and we found several structures within some dozens of kilojoules per mol for each complex. This means that it is probable that different conformations of the complexes are present simultaneously, especially at high temperatures like in the bleaching processes in which temperatures above 80°C are often used.

3.3. *Structural comparisons*

Six-coordinate structures **6b** of DTPA and HBDTTA are very close to octahedral geometry and the differences in structural parameters (bond lengths and angles) of Fe–DTPA and Fe–HBDTTA are relatively small. From the structural point of view, seven-coordinate structures are more interesting. Figure 4 shows a structural comparison for seven-coordinate $[Fe–DTPA]^{2-}$ and $[Fe–HBDTTA]^{2-}$. Metal–ligand bond lengths (in Angström) and selected bond angles (in degrees) between the structures are shown.

Both complexes are in distorted pentagonal bipyramidal geometry. As seen in figure 4, Fe–N bonds are slightly longer in $[Fe–HBDTTA]^{2-}$ with respect to $[Fe–DTPA]^{2-}$. Fe–O2 bond is clearly longer in $[Fe–HBDTTA]^{2-}$ and the bond angle N2–Fe–O2 smaller than the corresponding value in $[Fe–DTPA]^{2-}$, probably due to two effects: first, the large phenolate groups at both ends of the ligand cause general distortion to the ligand with respect to DTPA. For the same reason, the O1–Fe–O4

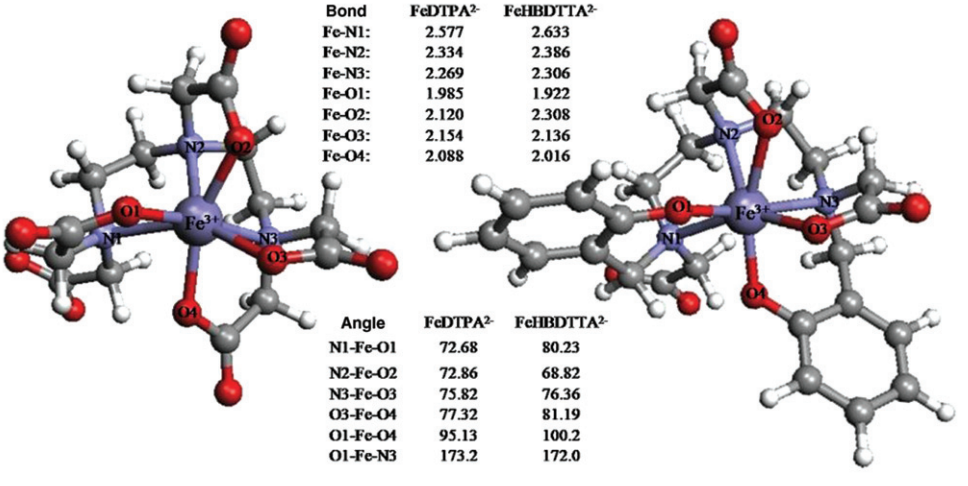

Figure 4. Metal–ligand bond lengths (in Angström) and bond angles (in degrees) in seven-coordinate $[Fe–DTPA]^{2-}$ and $[Fe–HBDTTA]^{2-}$.

angle is more than 5° larger in Fe–HBDTTA than in Fe–DTPA. Second, the phenol–oxygen bonds to Fe^{3+} are shorter than Fe–O1, and Fe–O4 bonds in Fe–DTPA, indicating stronger bonding, which weakens (i.e., lengthens) the other metal–ligand bonds. Overall Fe–HBDTTA is more distorted than Fe–DTPA, which partly explains the lower binding energy of seven-coordinate HBDTTA compared to DTPA. In general, COSMO model produces slightly longer bonds than those measured experimentally using crystal structures as seen previously, for example with ZnCys [20] and Fe–EDDHA [19] complexes. The ligand strain energies for these complexes have been calculated and the results are presented in section 3.5.

3.4. *Complexation energies*

Complexation energies have been calculated using equation (1). Table 1 shows the complexation energies for the most stable $[Fe–HBDTTA]^{2-}$, $[Fe–\mathbf{4c}]^{-}$, and $[Fe–\mathbf{5d}]^{-}$ complexes compared to the corresponding values of DTPA, HBED, EDTA, and *o*,*o*-EDDHA. Experimental values $\Delta G_{\text{experimental}}$ are shown (where available). ΔE_{C0} values indicate that the ligands *o*,*o*-EDDHA, **4c**, and HBED are the most effective chelators for Fe^{3+}. With respect to EDTA and DTPA, HBDTTA is expected to be a very efficient chelating agent. ΔE_{C0} for $[Fe–\mathbf{5d}]^{-}$ is *ca* 64 kJ mol^{-1} higher than ΔE_{C0} for $[Fe–\mathbf{4c}]^{-}$ but still *ca* 30 kJ mol^{-1} lower than the complexation energy for $[Fe–EDTA]^{-}$, and 17 kJ mol^{-1} lower than ΔE_{C0} for $[Fe–DTPA]^{2-}$.

The two ligand pairs HBDTTA–DTPA and HBED–EDTA have one thing in common, the first ligand is obtained by replacing two COOH groups of the latter by phenol. In the case of EDTA and HBED, this modification leads to an improvement of 85 kJ mol^{-1} (experimentally) and 95 kJ mol^{-1} (computationally) in complexation free energy. For DTPA and HBDTTA, on the other hand, the difference in experimental ΔG is only 14 kJ mol^{-1}. Computational results predict clearly larger enhancement (63 kJ mol^{-1}). To us, this discrepancy is strange, as in our calculations the two ligand

Table 1. Calculated (BP86/TZVP/COSMO) and experimental complexation free energies. $\Delta G_{\text{experimental}}$ have been derived from $\log K_1$ values for complexation at 0.1 ionic strength and 298 K using $\Delta G_{\text{experimental}} = -RT \ln 10 \log K_1$. All values are expressed in kilojoules per mol. Note that in experiments, the coordination number is not known and thus we used the same $\Delta G_{\text{experimental}}$ for all binding geometries.

Ligand	Coordination	ΔE_{C0}	ΔG_{C1}	$\Delta G_{\text{experimental}}$
HBDTTA	6a	−467	−183	−174[a]
DTPA	6a	−420	−136	−160[b]
HBDTTA	6b	−490	−206	−174[a]
DTPA	6b	−422	−138	−160[b]
HBDTTA	7	−468	−184	−174[a]
DTPA	7	−427	−143	−160[b]
4c	6	−508	−224	–
4c	7	−485	−201	–
5d	6	−444	−160	–
HBED	6	−507[c]	−223	−227[d]
EDTA	6	−413[c]	−129	−143[b]
o,*o*-EDDHA	6	−520[c]	−236	−200[e]

[a]Ref. [15]; [b]Ref. [32]; [c]Ref. [19]; [d]Ref. [33]; and [e]Ref. [34].

pairs behave analogously. This clearly demonstrates that the difficulty of predicting complexation behavior of a new ligand is just based on earlier experience on similar cases.

In general, calculated ΔE_{C0} deviate quite a lot from the $\Delta G_{experimental}$ and thus, further correction (in addition to the correction made by COSMO) is needed. In this study, we have applied the previously developed empirical correction parameter to correct for omitted contributions in "raw" ΔE_{C0} values. The parameter has been fitted with ΔE_{C0} and $\Delta G_{experimental}$ with several aminopolycarboxylate ligands, including, for example, EDTA and DTPA. For Fe^{3+}, correction is 284 kJ mol^{-1} [17]. Note that the designation of ΔG_{C1} has been changed with respect to the study of Sillanpää *et al.*

The value of ΔG_{C1} for $[Fe–HBDTTA]^{2-}$ is overestimated with respect to the experimental value. The same tendency has been seen with *o*,*o*-EDDHA and thus, also the ΔG_{C1} values for complexes of **4c** and **5d** can be considered optimistic. Aware of this probable but rather small inaccuracy, we rely more on the relative energies and on the general trend, which has been proven to reproduce the experimental binding trends.

To evaluate the possible inaccuracies that originate from the used GGA functional (BP86), we tested two hybrid functionals PBE0 and B3LYP for selected structures. The tested structures were six- and seven-coordinate structures of $[Fe–DTPA]^{2-}$ and $[Fe–HBDTTA]^{2-}$. ΔE_{C0} for the complexes obtained with different functionals are shown in table 2. All values are expressed in kilojoules per mol and they refer to BP86/TZVP/COSMO optimized geometry.

As seen in table 2, the calculated ΔE_{C0} are strongly dependent on the used functional. With respect to BP86, the values obtained with PBE0 are lower and those obtained with B3LYP are visibly higher (=less negative). Two important conclusions can be made based on data shown in table 2: (1) The trends in relative stabilities of the structures obtained with BP86 and PBE0 are equal. B3LYP, on the other hand, slightly favors the six-coordinate structures. (2) Despite the large differences in ΔE_{C0}, for all tested functionals, the deviation from $\Delta G_{experimental}$ (table 1) is notable and thus, further correction of the "raw" ΔE_{C0} is necessary.

3.5. *Strain energies*

An interesting observation about the energies presented in table 2 is that with BP86, the six- and seven-coordinate structures of DTPA and HBDTTA complexes

Table 2. Calculated complexation energies ΔE_{C0} (kJ mol^{-1}) for six- and seven-coordinate $[Fe–HBDTTA]^{2-}$ and $[Fe–DTPA]^{2-}$ complexes (**6a**, **6b**, and **7**) with different density functionals. All values refer to BP86/TZVP/COSMO optimized geometries (figure 3).

		ΔE_{C0}		
Ligand	Coordination	BP86	PBE0	B3LYP
HBDTTA	6a	−467	−476	−323
DTPA	6a	−420	−459	−264
HBDTTA	6b	−490	−541	−346
DTPA	6b	−422	−464	−266
HBDTTA	7	−468	−517	−280
DTPA	7	−427	−473	−258

(except [Fe–HBDTTA]$^{2-}$ **6a**) are almost equally stable. It is very likely that in the seven-coordinate structures, the electrostatic metal–ligand interactions are stronger and so there has to be another effect to compensate this. To study this, we calculated ligand strain energies for the selected complex structures of DTPA, HBDTTA, **4c**, and **5d**. For the first two ligands, both six- and seven-coordinate structures were considered. Strain energy E_{strain} is defined as

$$E_{strain} = E_{CSM}(L_{complex}) - E_{CSM}(L_{free}), \quad (3)$$

$E_{CSM}(L_{free})$ refers to the total energy of the COSMO optimized free ligand, while $E_{CSM}(L_{complex})$ is the total energy of the ligand in the complex structure. Strain energies for HBDTTA, DTPA, **4c**, and **5d** are presented in table 3.

In the first two six-coordinate complexes (**6a**) Fe–HBDTTA and Fe—DTPA, ligand strain energy is almost equal. In the **6b** structures, the difference in ligand strain energies is huge, *ca* 300 kJ mol^{-1} favoring the DTPA complex. Also, the seven-coordinate Fe–HBDTTA is more strained by 60 kJ mol^{-1} than the corresponding DTPA complex. The seven-coordinate structures of Fe–HBDTTA and Fe–**4c** are identical from the point of view of metal–ligand bonding pattern and thus, E_{strain} in these complexes are within 10 kJ mol^{-1}. The ligand **5d** has only one phenol ring and has strain energy comparable to E_{strain} of six-coordinate Fe–HBDTTA and Fe–DTPA.

The study of strain energies clearly shows that there are two competing effects related to complexation. First, there is the electrostatic attraction between the metal and donor groups of the ligand and second, there is the ligand strain energy. The calculation of the strain energies is straightforward. However, the study of the electrostatic attraction is more complicated because different donor atoms seem to have fairly different interaction energies with the metal. In order to increase our knowledge related to this phenomenon, we are currently studying the metal–ligand interactions more in detail.

4. Discussion

The members of the studied HBDTTA ligand family seem to be very effective complexing agents for Fe^{3+}. Their binding capacity is better than that of EDTA and DTPA and comparable to that of *o*,*o*-EDDHA or HBED. As HBED is obtained by

Table 3. Ligand strain energies (kJ mol^{-1}) in selected Fe–HBDTTA, Fe–DTPA, Fe–**4c**, and Fe–**5d** complexes.

Ligand	Coordination	E_{strain}
HBDTTA	6a	370
DTPA	6a	366
HBDTTA	6b	618
DTPA	6b	310
HBDTTA	7	463
DTPA	7	402
4c	6a	346
4c	7	455
5d	6	366

substituting two COOH groups of EDTA by phenolic rings, one could expect that similar effect can be seen when changing from DTPA to HBDTTA. Computationally, this effect is clear even if the experimental results predict smaller enhancement in $\log K$ values. Also the "incomplete" forms of HBDTTA, i.e., **4c** and **5d**, are predicted to be very effective chelators for Fe^{3+}. This makes HBDTTA-type ligands very interesting as these ligands can be modified by removing some of their functional groups without greatly affecting their binding capacities. For other ligands, modification can lead to more drastic changes on their binding behavior. This is the case for EDDHA, where repositioning of the phenolic OH group from *ortho* to *para* causes a change of *ca* $40\,kJ\,mol^{-1}$ in complexation energy [19].

Iron is a very effective catalyst for many reactions, for example for the dissociation of hydrogen peroxide. Chelating agents are often used to prevent the unwanted dissociation of H_2O_2. To be able to deactivate the metal ion, the ligand must shield the metal ion completely. Our calculations on the HBDTTA ligand family show that all the ligands (HBDTTA, **3b**, **4c**, **4d**, and **5d**) provide enough coordination sites to do this. This is in agreement with preliminary peroxide stabilization test results [35]. The results mean that the performance of a certain chelating agent cannot be predicted by considering only the $\log K_1$ values of its metal complexes. Possible impurities, synthesis side products, and isomerism are also factors that may have an effect on the ligands' overall behavior as stabilizer. This is the case for EDDHA, the most common synthesis route of which [36, 37] produces also *o*,*p*- and *p*,*p*-isomers of the ligand. These two isomers are rather effective chelating agents for Fe^{3+} but due to their under-coordinated complex structures [19], they are probably not able to inactivate the metal ion.

Although the absolute energies are inaccurate due to the used empirical correction, the relative energies are reliable and can be used to compare the binding capacity of different ligands for one metal ion. The study of geometries is of special importance in the case of Fe^{3+}, which can form metal complexes with coordination numbers from six to eight and often has more than one stable complexation geometry. As seen in this study, this kind of approach is more than helpful when the applicability of a certain ligand is studied.

5. Conclusions

Amino polycarboxylic acids are well-known for their capacity to form stable complexes with transition metal ions. Experimental methods provide techniques for determining the stability constants for complexation reactions. Some geometrical information can be obtained, for example from NMR experiments, and crystal structures can be measured with X-ray technique. However, also these methods have their limitations as several equilibrium reactions may occur simultaneously, and the crystal structures do not necessarily represent the solution structures of the complexes. Molecular modeling provides a fast approach for structural analysis without complicated experimental procedures. In this study, we have applied a previously developed and tested method, which has been shown to be suitable and powerful for this kind of applications. The ligands have been synthesized and their complexation properties predicted by DFT calculations at the BP86/TZVP level. The results indicate that like $[Fe–DTPA]^{2-}$,

$[Fe–HBDTTA]^{2-}$ also has several complex structures that are energetically close to each other, which may be a reason for its performance in peroxide stabilization tests. Other members of the HBDTTA ligand family are predicted to be efficient chelators for Fe^{3+} as long as they have enough (i.e., at least six) well-positioned coordination sites for complexation. Generally, based on geometry optimizations and complexation energy calculations, the following conclusions can be made for complexation of Fe^{3+} with HBDTTA-type ligands. The groups that coordinate to the metal ion include at least one phenolic group, two amino groups, and two carboxyl groups. Thus, the presence of these groups in the ligand is essential. The sixth (and seventh, if possible) coordination site of metal may be occupied by carboxyl, amino, or phenolic group. The study shows the power of molecular modeling when the structural properties of metal complexes are concerned.

Acknowledgments

The financial support of Academy of Finland, grant no. 116839 (HP), Finnish National Foundation of Technology and Kemira Oyj is gratefully acknowledged. CSC (the Finnish IT Center for Science) is acknowledged for providing computational resources.

References

[1] Z. Yang, M. D'Entremont, Y. Ni, A.R.P. Heiningen. *Pulp Pap. Can.*, **98**, T408–413 (1997).
[2] J. Basta, L. Holtinger, W. Hermansson, P. Lundgren. Metal management in TCF/ECF bleaching. In *Proceedings of the International Pulp Bleaching Conference*, Vancouver, Canada, 13–16 June, pp. 29–32 (1994).
[3] L. Lapierre, J. Bouchard, R.M. Berry, B. Van Lierop. *J. Pulp Pap. Sci.*, **21**, 269 (1995).
[4] M. Orama, H. Hyvönen, H. Saarinen, R. Aksela. *J. Chem. Soc., Dalton Trans.*, 4644 (2002).
[5] H. Hyvönen, M. Orama, H. Saarinen, R. Aksela. *Green Chem.*, **5**, 410 (2003).
[6] H. Hyvönen, M. Orama, P. Alén, H. Saarinen, R. Aksela, A. Parén. *J. Coord. Chem.*, **58**, 1115 (2005).
[7] H. Hyvönen, M. Orama, R. Arvela, K. Henriksson, H. Saarinen, R. Aksela, A. Parén, J. Jäkärä, I. Renvall. *Appita J.*, **59**, 142 (2006).
[8] H. Hyvönen, R. Aksela. *J. Coord. Chem.*, **60**, 901 (2007).
[9] H. Hyvönen, P. Lehtinen, R. Aksela. *J. Coord. Chem.*, **61**, 984 (2008).
[10] H. Hyvönen, R. Aksela. *J. Coord. Chem.*, **61**, 2515 (2008).
[11] R. Aksela, A. Parén, J. Jäkärä, I. Renvall. The overall performance of new diethanolamine derivatives as complexing agents in peroxide and peracetic acid bleaching of TCF pulp. In *Proceedings of the 11th ISWPC International Symposium on Wood and Pulping Chemistry*, Nice, France, 11–14 June, pp. 481–484 (2001).
[12] D. Swern. *Organic Peroxides*, Vol. II, pp. 497–503, Wiley-Interscience, New York (1970).
[13] F. L'Eplattenier, I. Murase, A.E. Martell. *J. Am. Chem. Soc.*, **89**, 837 (1967).
[14] A.E. Frost, H.H. Freedman, S.J. Westerback, A.E. Martell. *J. Am. Chem. Soc.*, **80**, 530 (1958).
[15] R. Ma, I. Murase, A.E. Martell. *Inorg. Chim. Acta*, **223**, 109 (1994).
[16] R.D. Hancock, I. Cukrowski, E. Cukrowska, G.D. Hosken, V. Iccharam, M.W. Brechbiel, O.A. Gansow. *J. Chem. Soc., Dalton Trans.*, **18**, 2679 (1994).
[17] A.J. Sillanpää, R. Aksela, K. Laasonen. *Phys. Chem. Chem. Phys.*, **5**, 3382 (2003).
[18] H. Pesonen, A. Sillanpää, R. Aksela, K. Laasonen. *Polymer*, **46**, 12653 (2005).
[19] H. Pesonen, R. Aksela, K. Laasonen. *J. Mol. Struct. (Theochem)*, **804**, 101 (2007).
[20] H. Pesonen, R. Aksela, K. Laasonen. *J. Phys. Chem. A*, **114**, 46 (2010).
[21] R. Ahlrichs, M. Bär, M. Häser, H. Horn, C. Kölmel. *Chem. Phys. Lett.*, **162**, 165 (1989).
[22] A.D. Becke. *Phys. Rev. A*, **38**, 3098 (1988).

[23] J.P. Perdew. *Phys. Rev. B*, **33**, 8822 (1986).
[24] K. Eichkorn, O. Treutler, H. Öhm, M. Häser, R. Ahlrichs. *Chem. Phys. Lett.*, **240**, 283 (1995).
[25] K. Eichkorn, O. Treutler, H. Öhm, M. Häser, R. Ahlrichs. *Chem. Phys. Lett.*, **242**, 652 (1995).
[26] J.P. Perdew, M. Ernzerhof, K. Burke. *J. Chem. Phys.*, **105**, 9982 (1996).
[27] A.D. Becke. *J. Chem. Phys.*, **98**, 5648 (1993).
[28] A. Klamt, G. Schüürmann. *J. Chem. Soc., Perkin Trans.*, **2**, 799 (1993).
[29] H. Pesonen, A. Sillanpää, R. Aksela, K. Laasonen. *Polymer*, **46**, 12641 (2005).
[30] H. Pesonen, R. Aksela, K. Laasonen. In preparation (2010).
[31] W.M. Coleman, L.T. Taylor. *Inorg. Chem.*, **10**, 2195 (1971).
[32] A.E. Martell, R.M. Smith (Eds), *Critically Selected Stability Constants of Metal Complexes*, Version 4.0, Texas A&M University, College Station, TX (1997).
[33] R.J. Motekaitis, A.E. Martell, M.J. Welch. *Inorg. Chem.*, **29**, 1463 (1990).
[34] F. Yunta, S. Garcia-Marco, J.J. Lucena, M. Gómez-Gallego, R. Alcázar, M.A. Sierra. *Inorg. Chem.*, **42**, 5412 (2003).
[35] R. Aksela. Unpublished results.
[36] H.E. Petree, H.L. Myatt, A.M. Jelenevsky. Preparation of phenolic ethylene diaminepolycarboxylic acids. US Patent 4130582.
[37] J.A.L. Julien, A. Aymard. Nouveau procédé de preparation de lácide ethylenediamine N,N′-bis(o-hydroxyphénylacétique) et de derives de celui-ci. European Patent 0331556 A2.